January 1992

TRACK STRUCTURE MODEL FOR DAMAGE TO MAMMALIAN CELL CULTURES DURING SOLAR PROTON EVENTS

Francis A. Cucinotta
NASA Langley Research Center, Hampton, VA, francis.cucinotta@unlv.edu

J. W. Wilson
NASA Langley Research Center, Hampton, VA

L. W. Townsend
NASA Langley Research Center, Hampton, VA

J. L. Shinn
NASA Langley Research Center, Hampton, VA

Robert Katz
University of Nebraska-Lincoln, rkatz2@unl.edu

Nucl. Tracks Radiat. Meas., Vol. 20, No. 1, pp. 177–184, 1992
Int. J. Radiat. Appl. Instrum., Part D
Printed in Great Britain

0735-245X/92 $5.00 + .00
Pergamon Press plc

TRACK STRUCTURE MODEL FOR DAMAGE TO MAMMALIAN CELL CULTURES DURING SOLAR PROTON EVENTS

F. A. CUCINOTTA,* J. W. WILSON,* L. W. TOWNSEND,* J. L. SHINN* and R. KATZ†
*Mail Stop 493, NASA Langley Research Center, Hampton, VA 23665–5225, U.S.A. and
†University of Nebraska, Lincoln, NE 68588–0150, U.S.A.

(*Received* 19 *February* 1991; *in revised form* 6 *May* 1991)

Abstract—Solar proton events (SPEs) occur infrequently and unpredictably, thus representing a potential hazard to interplanetary space missions. Biological damage from SPEs will be produced principally through secondary electron production in tissue, including important contributions due to delta rays from nuclear reaction products. We review methods for estimating the biological effectiveness of SPEs using a high energy proton model and the parametric cellular track model. Results of the model are presented for several of the historically largest flares using typical levels and body shielding.

1. INTRODUCTION

MANNED interplanetary space travel will involve long periods away from the protective cover of the Earth's magnetic field to regions where there exists the possibility of serious biological injury from galactic cosmic rays (GCRs) and energetic solar particle events (SPEs). Stochastic effects, most importantly cancer, are a concern for both GCRs and SPEs, while acute effects may become important during an SPE because of the possibility of large doses occurring during a period from several hours to days. Methods for describing GCR transport and interactions are described in a companion paper (Townsend *et al.*, 1992). In this paper, we describe transport methods and interactions of importance for SPEs and methods for describing biological effects.

Stochastic effects are expected to occur at low dose levels and low dose rates where only intratrack effects are important. Acute injury will only occur at dose levels sufficiently large for intertrack mechanisms. Recently, we have studied cellular response to high energy proton irradiations (Cucinotta *et al.*, 1991a) using the parametric cellular track model (Katz *et al.*, 1971). The effects of high energy protons in the intratrack regime were shown to proceed principally through the production of high linear energy transfer (LET) nuclear secondaries in tissue. At high doses, the nuclear secondary component was shown to be of less importance, and cumulative effects from primary protons were shown to be dominant. A second topic of this paper is to study cellular response from large SPEs using the cellular track model. We consider cell survival and neoplastic transformation of C3H10T1/2 mouse cell cultures as an illustration of acute and stochastic processes at the cellular level.

We next give a brief overview of the occurrence of large solar-particle events. Transport methods and interactions of importance for SPEs as contained in the BRYNTRN (baryon transport) model (Wilson *et al.*, 1989a) are then described. Finally, the application of the track model to SPEs is considered for several major events, and our results are discussed.

2. SOLAR PROTON EVENTS

Solar flares are associated with the sun and solar activity. There are a large number of optical flares in which radio bursts and plasma are ejected. For a very few of these flares, high energy particles are also ejected into interplanetary space. Particles are able to escape the solar magnetic fields only if the field lines are open to the interplanetary region. These events are dominated by the ejection of protons, however, alpha particles and heavy ions have also been detected (Shea and Smart, 1990). The composition of those heavier nuclei is not well known and predictions of biological effects generally refer only to protons (also see Curtis *et al.*, 1966). Shea and Smart (1990) have summarized the experimental data for all proton events with at least 10 particles $cm^{-2}\,s^{-1}\,sr^{-1}$ above 10 MeV, for the last three solar cycles. The largest events may have as many as 10^9–10^{10} particles above 10 MeV. For radiation assessment, the distribution in particle energy becomes important, since the particles must penetrate through spacecraft shielding. In this paper, we consider three anomalously large events; those of February 1956, August 1972 (Wilson and Denn, 1976), and October 1989 (Sauer *et al.*, 1990). The cumulative spectra of particles for these events are represented by the curves in Fig. 1. The 1956

event contains the largest number of highly penetrating particles.

The temporal development of a proton event will be extremely important for initiating evasive countermeasures and for understanding biological effects. Solar protons will arrive at the Earth within several minutes for relativistic particles and longer times, perhaps hours, for particles of lower energy (Shea and Smart, 1990). Detection at the Earth does not preclude propagating along other field lines, and a warning system for interplanetary travelers may not be possible. Events will typically occur over periods of several hours to days. We refer to the work of Feynman *et al.* (1988) for methods of predicting the onset of an event, and of Townsend *et al.* (1991) and Nealy *et al.* (1990) for temporal analyses. Cellular repair processes occur for time periods of less than a few hours and are especially effective for low LET radiations. The importance of repair processes will have to be understood for any complete description of SPE potential hazards.

3. PROTON AND SECONDARY PARTICLE TRANSPORT

3.1. *Transport equations*

In moving through bulk material, protons give up energy to the medium through atomic/molecular and nuclear interactions. The produced secondary nuclear particles from collisions will also suffer energy losses and become part of the transport problem. The importance of secondary electron production as related to biological response is considered below. The transport of ions is described by Boltzmann-like equations (Wilson *et al.*, 1989a), which in the straightahead approximation are written

$$\left[\frac{\partial}{\partial x}-\frac{\partial}{\partial E}S(E)+\sigma_p(E)\right]\phi_p(x,E)=\sum_j\int_E^\infty f_{pj}(E,E')\phi_j(x,E')\,dE' \quad (1)$$

$$\left[\frac{\partial}{\partial x}+\sigma_n(E)\right]\phi_n(x,E)=\sum_j\int_E^\infty f_{nj}(E,E')\phi_j(x,E')\,dE' \quad (2)$$

$$\left[\frac{\partial}{\partial x}-\frac{\partial}{\partial E}\nu_t S(E)\right]\phi_t(x,E)=\sum_j\int_0^\infty f_{tj}(E,E')\phi_j(x,E')\,dE' \quad (3)$$

where $\phi_j(x,E)$ is the differential flux density of type j particle at x with energy E; $S(E)$ is the proton stopping power; ν_t is the ion-range scaling parameter; $\sigma_p(E)$ and $\sigma_n(E)$ are proton and neutron total cross-sections, respectively; and $f_{ij}(E,E')$ represents the differential cross-sections for elastic and non-elastic

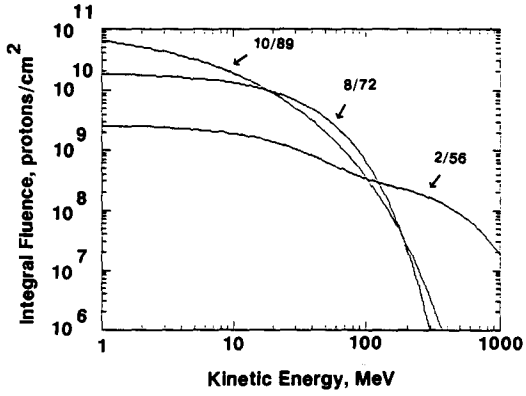

FIG. 1. Integral fluence spectra as a function of particle kinetic energy for three major solar particle events.

processes. It is convenient to define new field quantities as

$$r=\int_0^E dE'/S(E') \quad (4)$$

$$\psi_j(x,r)=S(E)\phi_j(x,E) \quad (5)$$

$$\bar{f}_{ij}(r,r')=S(E)f_{ij}(E,E') \quad (6)$$

so that

$$\left[\frac{\partial}{\partial x}-\frac{\partial}{\partial r}+\sigma_p(r)\right]\psi_p(x,r)=\sum_j\int_r^\infty \bar{f}_{pj}(r,r')\psi_j(x,r')\,dr' \quad (7)$$

$$\left[\frac{\partial}{\partial x}+\sigma_n(r)\right]\psi_n(x,r)=\sum_j\int_r^\infty \bar{f}_{nj}(r,r')\psi_j(x,r')\,dr' \quad (8)$$

$$\left[\frac{\partial}{\partial x}-\nu_j\frac{\sigma}{\partial_r}\right]\psi_t(x,r)=\sum_j\int_0^\infty \bar{f}_{tj}(r,r')\psi_j(x,r')\,dr' \quad (9)$$

which can be rewritten as integral equations with the boundary at $x=0$. The following results are given:

$$\psi_p(x,r)=\exp\left[-\int_0^x\sigma_p(r+z)\,dz\right]\psi_p(0,r+x)+\int_0^x dz\,\exp\left[-\int_0^z\sigma_p(r+w)\,dw\right]\times\sum_j\int_{r+z}^\infty\bar{f}_{pj}(r+z,r')\psi_j(x-z,r')\,dr' \quad (10)$$

$$\psi_n(x,r)=\exp[-\sigma_n(r)x]\psi_n(0,r)+\int_0^x dz\,\exp[-\sigma_n(r)z]\times\sum_j\int_r^\infty\bar{f}_{nj}(r+r')\psi_j(x-z,r')\,dr' \quad (11)$$

$$\psi_t(x, r) = \int_0^x \mathrm{d}z \sum_j \int_0^\infty \bar{f}_{ij}(r + v_t s, r') \times \psi_j(\chi - z, r')\,\mathrm{d}r'. \quad (12)$$

Equations (10)–(12) are solved using numerical procedures to propagate the solution from the boundary at $x = 0$ as described by Wilson *et al.* (1989a).

For nuclear secondaries with mass numbers $A \geqslant 2$, the probability for nuclear collisions are small, since these ions will be of low energy, typically only a few MeV. The differential flux for these ions can then be solved in closed form for the target fragments with $A \geqslant 2$ as in Wilson (1977)

$$\phi_j(x, E) = \frac{1}{S_j(E)} \int_E^\infty f_{pj}(E, E')\phi_p(x, E)\,\mathrm{d}E' + \frac{1}{S_j(E)} \int_E^\infty f_{nj}(E, E')\phi_n(x, E)\,\mathrm{d}E' \quad (13)$$

where the first and second terms in (13) correspond to ions produced by protons and neutrons, respectively. The largest uncertainties expected in the transport algorithms contained in BRYNTRN are expected to be the treatment of neutrons, especially at low energies. Improvements in this area are expected in the near future.

3.2. *Stopping powers*

In passing through a material, an ion loses a substantial fraction of its energy to electronic excitation of the material. For energies greater than a few MeV per nucleon, Bethe's theory using the Born approximation is adequate provided appropriate corrections to Bragg's rule, shell corrections, and effective charge are included (Wilson, 1983). Proton stopping powers are taken from the parametric expressions of Anderson and Ziegler (1976). A modification to their shell corrections, however, has been added to ensure a smooth transition to Bethe's asymptotic formula.

For alphas, the electronic stopping power is not derivable from proton stopping power at low energies because of the neglect of higher-order Born terms. Instead, the parametric fits to experimental data, given by Ziegler (1977b) are used. Electronic stopping powers S_j for ions of charge greater than two are scaled to the alpha stopping powers.

At sufficiently low energies, the energy lost by the ion because of nuclear collisions becomes important. The nuclear stopping theory used herein is a modified form (Ziegler, 1977a) of the theory of Linhard *et al.* (1963). The total stopping power is obtained by summing electronic and nuclear components.

3.3. *Nuclear interaction data base*

The transport description requires an extensive nuclear cross-section data base. All elastic and non-elastic cross-sections, both integral and differential in energy, must be represented for protons and neutrons in arbitrary shielding materials, and over several decades in energy. For computational efficiency, the data base is provided by analytic functions, whenever possible, that are representative of available experimental data or Monte Carlo calculations when data are not available. Here we give a brief description of some of the many nuclear inputs.

Inelastic processes are described by the absorption cross-section and the production cross-sections for individual secondaries. A detailed description of the absorption cross-sections is given in the companion paper by Townsend *et al.* (1992). The production of light ions is based largely on Bertini's MECC-7 program [Bertini (1968) and Alsmiller *et al.* (1968)] with some modifications based on the model of Ranft (1980) to take into account low energy cascade particles.

The heavy fragment spectrum is based on the Goldhaber formalism (Goldhaber, 1974). Following direct ejection of nucleons in a collision, the nucleus is assumed to be left in a highly excited state that decays through particle emission. The momentum distribution of fragments is expected to be governed by the Fermi distribution prior to the collision. Goldhaber (1974) provides an adequate model for the random decay of these excited states. The momentum distribution for fragment production is Gaussian in momentum space with a momentum width parameter given by

$$\sigma_p = \sigma_0[A_t - A_f)/(A_t - 1)]^{1/2} \quad (14)$$

where σ_0 is the usual mean Fermi momentum of the struck nucleus. However, the σ_0 of nuclear fragmentation is found to be about 25% smaller than that observed in electron-scattering experiments. The mean Fermi momentum is a slowly varying function of nuclear mass.

A slight modification of Goldhaber's result is found to adequately represent the experimental results of Greiner *et al.* (1975) given by

$$\sigma_p = 0.8\mathrm{b}[4\delta_A/20(A_t - 1)]^{1/2} \quad (15)$$

where parameters b and δ_A are given, respectively, by

$$b = \min(112A_t^{1/2}, 260) \quad (16)$$

and

$$\delta_A = \begin{cases} 0.45 & (A_t = A_f) \\ A_t - A_f & (\text{otherwise}) \end{cases}. \quad (17)$$

The spectral distributions of the nuclear fragments in the rest frame of the struck nucleus prior to collision are given by

$$\frac{\mathrm{d}\sigma_f}{\mathrm{d}E} = \frac{\sigma_f}{(2\pi E_0^3)^{1/2}} E^{1/2} \exp(-E/2E_0) \quad (18)$$

where σ_f is the fragmentation cross-section and the energy parameter is

$$E_0 = 3\sigma_p^2/2A_f. \quad (19)$$

The fragmentation cross-sections are based on a modified form of Rudstam's results, which are based on studies of the systematics of spallation products (Rudstam, 1966) and which assume that isotopes are distributed in a bell-shaped distribution near the nuclear stability line. Corrections are described by Wilson *et al.* (1989a,b). The importance of nuclear reactions results from their production of high LET components within biological systems. The LET spectra of 1 GeV proton-induced nuclear events are shown in Fig. 2.

4. CELLULAR TRACK MODEL

The cellular track model of Katz has been described extensively (Katz *et al.*, 1971, 1972). Here we outline its basic concepts and discuss the inclusion of target fragmentation contribution for proton irradiations. Biological damage by ions is assumed to be principally caused by delta ray production along the ions' path. Cell inactivation is separated into a grain-count regime, where inactivation occurs randomly along the path of the particle and into the track-width regime, where many inactivations occur and are said to be distributed like a "hairy rope". Four cellular parameters describe the response of the cells, two of which (m, the number of targets per cell; and D_0, the characteristic X-ray dose) are extracted from the response of the cellular system to X- and γ-ray irradiation. The other two (σ_0 interpreted as the cross-sectional area of the cell nucleus within which the inactivation sites are located; and κ, a measure of the size of the inactivation site) are found from survival measurements with track segment irradiations by charged particles. The transition from the grain-count regime to the track-width regime takes place at about $Z^{*2}/\kappa\beta^2$ of about 4; at lower values we are in the grain-count regime and at higher values the track-width regime.

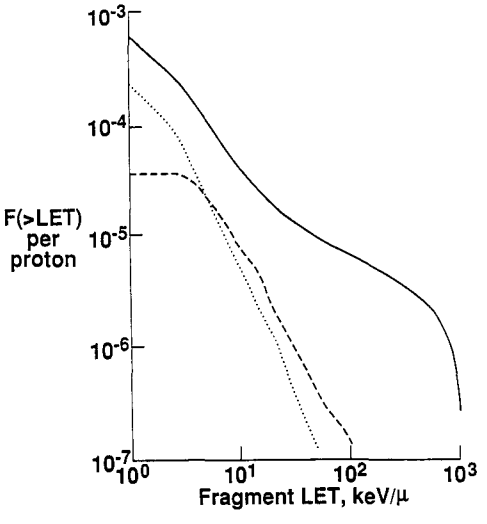

FIG. 2. Integral LET spectra for nuclear fragments produced by 1 GeV protons in water. Solid line, all fragments; dotted line, secondary protons; dashed line, secondary alpha particles.

To accommodate for the capacity of cells to accumulate sub-lethal damage, two modes of inactivation are identified: ion-kill (intratrack) and gamma-kill (intertrack). When the passage of a single ion damages cells, the ion-kill mode occurs. In the grain-count regime, the fraction of cells damaged in the ion-kill mode is taken as $P = \sigma/\sigma_0$, where σ is the single particle inactivation cross-section and P is the probability of inactivation in the ion-kill mode. Delta rays from the passing ion can sublethally damage cells not inactivated in the ion-kill mode. Cumulatively adding sublethal damage due to delta rays from other passing ions can inactivate these cells in the gamma-kill mode. The surviving fraction of a cellular population N_0, whose response parameters are m, D_0, σ_0, and κ after irradiation by a fluence of particles F, is written (Katz *et al.*, 1971)

$$\frac{N}{N_0} = \pi_i \times \pi_\gamma \tag{20}$$

where the ion-kill survivability is

$$\pi = e^{-\sigma F} \tag{21}$$

and the gamma-kill survivability is

$$\pi_\gamma = 1 - (1 - e^{-D_\gamma/D_0})^m. \tag{22}$$

The gamma-kill dose fraction is

$$D_\gamma = (1 - P)D \tag{23}$$

where D is the absorbed dose. The single particle inactivation cross-section σ is taken in the grain-count regime as

$$\sigma = \sigma_0(1 - e^{Z^{*2}/\kappa\beta^2})^m \tag{24}$$

where the effective charge number is given by

$$Z^* = Z(1 - e^{-125\beta/z^{2/3}}). \tag{25}$$

In the track-width regime, we use the approximation from Roth and Chang (1977)

$$\sigma = \sigma_0\left\{1 + (C_1 + C_2 m + C_3 m^2)\left(\frac{Z^{*2}}{\kappa\beta^2}\right)^{1.4}\right\} \tag{26}$$

where $C_1 = 0.0393517$, $C_2 = -0.130822$, and $C_3 = 0.00137756$, which allows for $\sigma > \sigma_0$ but does not represent the "hook" structure observed for very high LET ions.

The RBE at a given survival level is given by

$$\text{RBE} = D_x/D \tag{27}$$

where

$$D_x = -D_0 \ln[1 - (1 - N/N_0)^{1/m}] \tag{28}$$

is the X-ray dose at which this survival level is obtained. Of particular interest is the low fluence limit of equation (28). When gamma-kill does not

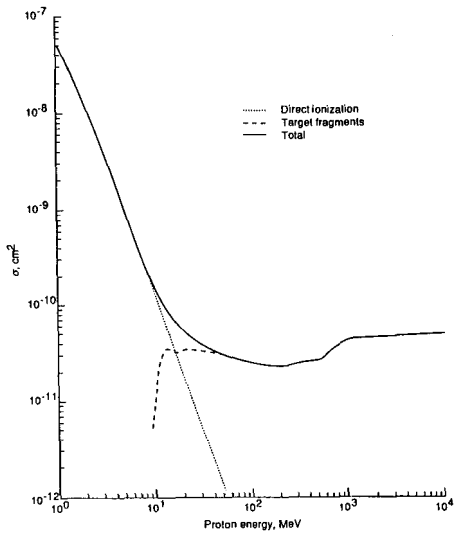

FIG. 3. Proton action cross-section for survival of C3H10T1/2 cells. Solid line, total; dotted line, direct ionization; dashed line, target fragments.

contribute, $D \ll D_0$, and only single track effects occur, so that equation (27) is approximately

$$\mathrm{RBE} = D_0\left(\frac{\sigma}{\mathrm{LET}}\right)^{1/m} D^{(1/m-1)} \qquad (29)$$

(Katz and Cucinotta, 1991).

We next extend the track model to include the effects of target fragmentation in tissue.

High energy protons passing through tissue will occasionally suffer nuclear reactions that produce low energy, high LET ions from the tissue itself (see Fig. 2). The target fragments, in turn, will be a source of delta ray production leading to additional inactivations along the tissue matrix. The ion-kill function

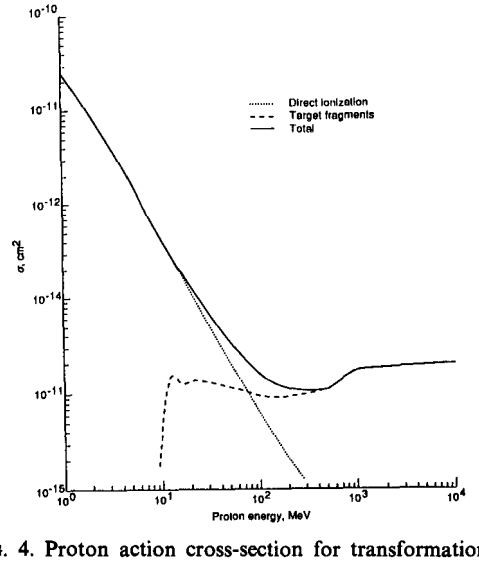

FIG. 4. Proton action cross-section for transformation of C3H10T1/2 cells. Solid line, total; dotted line, direct ionization; dashed line, target fragments.

for a distribution of protons and their secondaries is written

$$\sigma F = \int_0^\infty \sigma_p(E_p)\phi_p(x, E_p)\,\mathrm{d}E_p + \sum_j \int_0^\infty \int \sigma_j(E)\phi_j(x, E;\, E_p)\,\mathrm{d}E\,\mathrm{d}E_p \qquad (30)$$

where the second term in equation (30) is from the target fragments. The relative contribution of target fragments is shown in Figs 3 and 4 in comparison with the direct ionization term of equation (30). Secondary neutrons will also contribute to biological effects through reaction products and these contributions are estimated by the second term in equation (30) at higher energies (> 10 MeV). Low energy neutrons are expected to be important, especially for thick spacecraft shielding, but are not considered here. The gamma-kill function now becomes

$$D_\gamma = \int_0^\infty \mathrm{d}E_p \phi(x, E_p)(1 - P_p(E_p)) + \sum_j \int_0^\infty \int_{E_p}^\infty \mathrm{d}E\,\mathrm{d}E_p \times \phi_j(x, E, E_p)(1 - P_j(E_j)). \qquad (31)$$

The second term in (31) is found to be small (Cucinotta *et al.*, 1991a,b) indicating that secondary ions do not contribute through intertrack action. Predictions will be made for cell death (loss of reproductive capability) and neoplastic transformations of C3H10T1/2 cells. The response parameters of Table 1 were found from the delayed plating experiments of Yang *et al.* (1985) and Waligorski *et al.* (1987).

5. RESULTS AND DISCUSSION

In Fig. 2, we show calculations of the secondary integral LET fluence spectra for 1 GeV protons in water. The solid line is the total, and the dotted line and dashed line show individual contributions for protons and alphas, respectively. Ions are produced over a large range of LET values, but only a small number of particles are produced per proton. That secondary ions dominate the biological effect can be seen in Figs 3 and 4 where calculations of the effective cross-sections for survival and transformation of C3H10T1/2 cells are shown vs the proton energy (Cucinotta *et al.*, 1991b).

In Table 2, we show results of the track model for 3 g cm^{-2} of aluminum plus 5 g cm^{-2} of water shielding for three major flares. The harder 1956 event

Table 1. Cellular response parameters for C3H10T1/2 cells

Cell-damage type	m	D_0, cGy	σ_0, cm^2	κ
Death	3	280	5.0×10^{-7}	750
Transformation	2	26,000	1.15×10^{-10}	750

Table 2. C3H10T1/2 cell response for major solar proton event

	Fraction cells killed			Fraction cells transformed		
Event	Primary	Secondary	Total	Primary	Secondary	Total
Feb. 56	0.012	0.013	0.025	9.7×10^{-6}	5.5×10^{-6}	1.51×10^{-5}
Aug. 72	0.095	0.028	0.114	7.9×10^{-5}	1.2×10^{-5}	9.2×10^{-5}
Oct. 89	0.051	0.018	0.069	0.8×10^{-5}	0.8×10^{-5}	5.0×10^{-5}

shows the largest contribution from secondary particles where they make up more than half of the contribution to cell death (loss of cell reproductive capability). The August of 1972 event is dominated by primary particles and would be considered life-threatening if the response of cell cultures were close to those in tissue. In Figs 5 and 6, we show an integral LET spectra for cell death and transformation by the 1956 flare.

Finally, we would like to discuss predictions of RBEs for the major proton events. The RBE is expected to be an increasing function for decreasing dose (Katz and Cucinotta, 1991; Cucinotta *et al.*, 1991a). For Chinese hamster cells, we have found that secondaries give a modest increase above a value of unity to the RBE above doses of several Gy. At lower doses, the RBE increases as found in calculations (Cucinotta *et al.*, 1991a) and in experiments with 160 MeV protons (Hall *et al.*, 1979). Predictions for RBEs for the 1972 event are shown in Table 3a, b where we also list our calculated values of the average ICRP-26 (1977) quality factor. Increases in shielding correspond to decreases in dose and a rising RBE. The RBE for the more important transformation endpoint is seen to be the largest in our comparisons and substantially higher than QFs for thick shields.

6. CONCLUDING REMARKS

A brief description of the Langley Research Center transport code (BRYNTRN) has been presented. Methods for describing nuclear reactions in the transport algorithms and the interaction parameters were

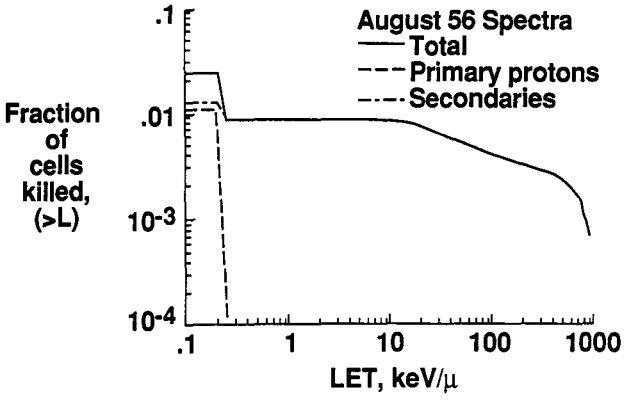

FIG. 5. Integral LET spectra for cell death of C3H10T1/2 cells from 1956 SPE behind 3 g cm^{-2} of Al plus 5 g cm^{-2} of water shielding. Solid line, total; dashed line, primary protons; dash–dot line, secondaries.

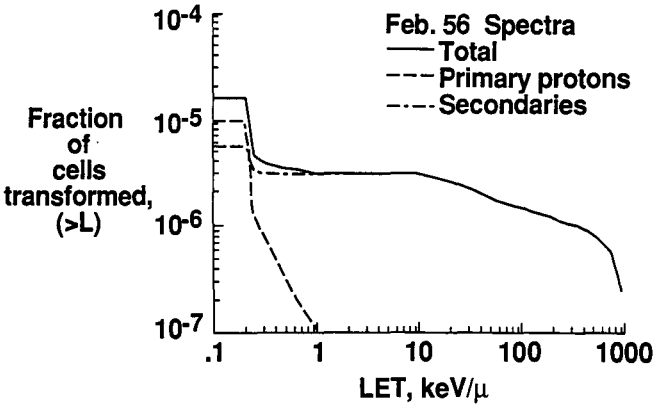

FIG. 6. Integral LET spectra for transformation of C3H10T1/2 cells from 1956 SPE behind 3 g cm^{-2} of Al and 5 g cm^{-2} of water. Solid line, total; dashed line, primary; dash–dot line, secondaries.

Table 3a. Comparison of RBEs for C3H10T1/2 cells vs ICRP-26 QFs for August 1972 event (5 g cm^{-2} of Al shielding)

x, g cm^{-2} of H_2O	D, cGy	QF	RBE for survival	RBE for transformation
0	528	1.6	0.7	0.9
1	356	1.5	0.8	1.0
2	256	1.5	0.9	1.2
3	189	1.5	1.0	1.3
5	110	1.5	1.3	1.7

Table 3b. Comparison of RBEs for C3H10T1/2 cells vs ICRP-26 QFs for August 1972 event (10 g cm^{-2} Al shielding)

x, g cm^{-2} of H_2O	D, cGy	QF	RBE for survival	RBE for transformation
0	152	1.5	1.2	1.6
1	108	1.5	1.3	1.7
2	83	1.5	1.5	1.9
3	65	1.5	1.7	2.1
5	41	1.6	2.2	2.6

discussed. Improvements in the low energy neutron transport were indicated as the principal objective of future work.

The coupling of the track model of Katz to the BRYNTRN code is discussed, and results for the cell death (loss of cell reproductive capability) and transformation of C3H10T1/2 cells are presented for three major SPEs. The relationship between *in vitro* and *in vivo* effects is not well known; however, our results may be considered alarming. There are about 10^9 cells per cm^3 of tissue with our results, indicating between 10^4 and 10^5 cells transformed per cm^3. Since it is the number rather than the fraction of transformed cells which is relevant to cancer induction, this fraction must be multiplied by the number of cells in the body capable of being transformed. Additionally, we recognize that the scaling from mouse cells *in vitro* to human cells *in vivo* is cloudy, but these results should flag a potential problem. Note that the predicted RBEs for cell transformation are substantially greater than the calculated quality factors. Target fragments were seen to make up a substantial fraction of the damage from SPEs. Improvements for future work in applications of the track model include adding the effects of low energy neutrons and modeling cellular repair processes as they relate to the temporal development of SPE.

REFERENCES

Alsmiller T. G. Jr, Barish J. and Leimdorfer M. (1968) Analytic representation of nonelastic cross sections and particle-emission spectra from nucleon–nucleus collisions in the energy range 25 to 400 MeV. Protection against space radiation, pp. 495–515. NASA SP-619.

Andersen H. H. and Ziegler J. F. (1976) *Hydrogen Stopping Powers and Ranges in All Elements*. Pergamon Press, New York.

Bertini H. W. (1968) MECC-7 Intranuclear cascade code, 500 MeV protons and 0-16 14C analysis codes available from radiation shielding information center, Oak Ridge National Laboratory, Oak Ridge, TN.

Cucinotta F. A., Katz R., Wilson J. W., Townsend L. W., Nealy J. E. and Shinn J. L. (1991b) Cellular track model of biological damage to mammalian cell cultures from galactic cosmic rays. NASA Technical Paper, Washington, DC, NASA TP-3055.

Cucinotta F. A., Katz R., Wilson J. W., Townsend L. W., Shinn J. L. and Hajnal F. (1991a) Biological effectiveness of high-energy protons: target fragmentation. *Radiat. Res.* **127,** 130–137.

Curtis S. B., Dye D. L. and Sheldon W. R. (1966) Hazard from highly ionizing radiation in space. *Health Phys.* **12,** 1069–1075.

Feynman J., Armstrong T. P. and Dao-Gibner L. (1988) A new proton fluence model for $E > 10$ MeV. *Proc. Conf. Interplanet. Part. Envir.* JPL Publication 88-028, 58-71.

Goldhaber A. S. (1974) Statistical models of fragmentation processes. *Phys. Lett.* **53B,** 306–308.

Greiner D. E., Lindstrom P. J., Heckman H. H., Cork B. and Bieser F. S. (1975) Momentum distribution of isotopes produced by fragmentation of relativistic ^{12}C and ^{16}O projectiles. *Phys. Rev. Lett.* **35,** 152–155.

International Commission on Radiological Protection—ICRP (1977) Recommendations of the Commission. ICRP Publication 26. Pergamon Press, New York.

Hall E. J., Kellerer A. M., Rossi H. H. and Lam Y. P. (1979) The relative biological effectiveness of 160 MeV protons—I. *Int. J. Radiat. One. Bio. Phys.* **4,** 1007–1013.

Katz R., Ackerson B., Homayoonfar M. and Sharma S. C. (1971) Inactivation of cells by heavy ion bombardment. *Radiat. Res.* **47,** 402–425.

Katz R. and Cucinotta F. A. (1991) RBE versus dose for low doses of high LET radiations. *Health Phys.* **60,** 717–718.

Katz R., Sharma S. C. and Homayoonfar M. (1972) The structure of particle tracks. In: *Tropics in Radiation Dosimetry* (Edited by Attix F. H.). Academic Press, New York.

Linhard J., Scharff M. and Schiott H. E. (1963) Range concepts and heavy ion ranges (notes on atomic collisions II). *Mat. Fys. Medd. Dan. Vid. Selsk.* **33,** 1–42.

Nealy J. E., Simonsen L. C., Townsend L. W. and Wilson J. W. (1990) Deep-space radiation exposure analysis for solar cycle XXI (1975–1986). *ICES Conf.*, Williamsburg, VA.

Ranft J. (1980) *The FLUKA and CASPRO Hadronic Cascade Codes. Computer Techniques in Radiation Transport and Dosimetry* (Edited by Nelson W. F. and Jenkins T. M), pp. 339–371. Plenum Press, New York.

Roth and Chang (1977) Private communication.

Rudstam G. (1966) Systematics of spallation yields. *Z. Naturforschung* **21a,** 1027–1041.

Shea M. A. and Smart D. F. (1990) A summary of major solar proton events. *Solar Phys.* **127,** 297–320.

Sauer H. H., Zwicki R. O. and Vess M. J. (1990) Summary data for the solar energetic particle events of August through December 1989. NOAA—Space Environmental Laboratory Report (unnumbered).

Townsend L. W., Wilson J. W., Cucinotta F. A. and Shinn J. L. (1992) Galactic cosmic ray transport methods and radiation quality issues. *Nucl. Tracks Radiat. Meas.* **20,** 65–72.

Townsend L. W., Wilson J. W., Shinn J. L. and Curtin (1991) Human exposure to large solar particle events in space. *Adv. Space Res.* (in press).

Waligorski M. P. R., Sinclair G. L. and Katz R. (1987) Radiosensitivity parameters for neoplastic transformations in C3H10T1/2 cells. *Radiat. Res.* **111,** 424–437

Wilson J. W. (1977) Analysis of the theory of high-energy ion transport. NASA TND-8381.

Wilson J. W. (1983) Heavy ion transport in the straight-ahead approximation. NASA Technical Paper, Washington, DC, NASA TP-2178.

Wilson J. W. and Denn F. M. (1976) Preliminary analysis of the implications of natural radiations on geostationary orbits. NASA Technical Note, Washington, DC, NASA TNO-8290.

Wilson J. W., Townsend L. W. and Khan F. (1989b) Evaluation of highly ionizing components in high-energy nucleon radiation fields. *Health Phys.* **57**, 717–724.

Wilson J. W., Townsend L. W., Nealy J. E., Chun S. Y., Hong B. S., Buck W. W., Lamkin S. L., Ganapol B. D., Khan F. and Cucinotta F. C. (1989a) BRYNTRN: a baryon transport model. NASA Technical paper, Washington, DC, NASA TP-2887.

Yang T. C., Craise L., Mei M. T. and Tobias C. A. (1985) Neoplastic cell transformation by heavy charged particles. *Radiat. Res.* **104**, S177–S187.

Ziegler J. F. (1977a) The electronic and nuclear stopping of energetic ions. *Appl. Phys. Lett.* **31**, 544–546.

Ziegler J. F. (1977b) *Helium Stopping Powers and Ranges in All Elemental Matter.* Pergamon Press, New York.